Time-dependent quantum transport behavior through T-shaped double quantum dots

2009 J. Phys.: Condens. Matter 21 265501

(http://iopscience.iop.org/0953-8984/21/26/265501)

IOP Publishing Journal of Physics: Condensed Matter

J. Phys.: Condens. Matter **21** (2009) 265501 (7pp) doi:10.1088/0953-8984/21/26/265501

Time-dependent quantum transport behavior through T-shaped double quantum dots

Hui Pan[1] **and Yinghui Zhao**[2]

[1] Department of Physics, Beijing University of Aeronautics and Astronautics, Beijing 100083, People's Republic of China
[2] Department of Electrical and Computer Engineering, Colorado State University, Fort Collins, CO 80523, USA

Received 5 November 2008, in final form 20 March 2009
Published 3 June 2009
Online at stacks.iop.org/JPhysCM/21/265501

Abstract

The time-dependent current flowing through a T-shaped double quantum dot is theoretically studied via nonequilibrium Green's function methods. Quantum coherent ringing or beats can appear in the transient current after a bias voltage is turned on or off, and their periods can be tuned by the pulse bias or the interdot coupling strength. In the weak interdot coupling case no quantum beat is observed and only quantum ringing appears in the current, the frequency of which depends on the pulse bias. In the strong interdot coupling case, quantum beats appear in the current and their frequency depends on the interdot coupling strength. Quantum beats are suppressed greatly by the large energy difference between the two quantum dots. In addition, quantum ringing and beats tend to disappear with increasing temperature.

(Some figures in this article are in colour only in the electronic version)

1. Introduction

Recently, the quantum transport property of quantum dot (QD) systems has become an active research field due for both purely fundamental reasons and possible applications in nanoelectronic devices. When an external ac field is applied to a QD system, the quantum transport becomes time dependent and one of the essential features is the well-known photon-assisted tunneling (PAT). Observations of PAT in single QD systems have been reported experimentally [1–3]. The electron can tunnel through the system by emitting or absorbing multiple photons, and then new inelastic tunneling channels are opened. Recently, the time-dependent current through a QD in the Kondo regime with strong Coulomb interaction has been theoretically studied, and the current has been shown to significantly depart from the noninteracting one and the Kondo resonance appears at the Fermi energy [22]. Another important issue is how fast a device can turn a current on (or off) under an ac signal due to the need to design a viable switching device [4]. Since the step or pulsed ac signals can provide a less ambiguous measure of timescales, time-dependent transport under a pulsed field was studied in a single QD [5–9] or nanostructure [10, 11]. Quantum coherent ringing (oscillations) of the current flowing through a QD was predicted after a bias voltage is turned on [7–10]. In addition to quantum coherent ringing, quantum beats of the spin-dependent current through a QD with Zeeman split levels were also predicted [12].

As well as the single QD system, parallel-coupled double quantum dot (DQD) systems have also been studied [13–15]. The interference effect between QD1 and QD2 plays an important role, and the linear conductance has an asymmetric line shape of the Fano resonance. Time-dependent tunneling through coupled DQDs in series has received a large amount of attention both experimentally and theoretically. Experimentally, the PAT current through serially-coupled DQDs has been observed, and the predicted extra resonance peaks under microwave irradiation are clearly seen [16, 17]. Theoretically, studies of the PAT in serially-coupled DQDs predicts that the photon response of the system will exhibit satellite resonance peaks due to PAT processes [18, 19], and a pumping current will also be found [20]. The main feature of the transport is that the electron keeps the phase coherence when traversing through the device in the nanometer scale. The phase of the tunneling electrons can be affected differently when the time-dependent field is applied in different parts of

the system. Other quantum structures, such as a side-coupled quantum dots, have also been reported in experiments [21].

However, the transport properties with the interplay of the ac field and quantum interference in a T-shaped DQD device have not been fully investigated. Therefore it is the purpose of this paper to study the time-dependent current through a T-shaped DQD connected with two normal leads. For simplicity, the Coulomb interaction is neglected. In the Coulomb blockade regime with low Coulomb interaction the current is qualitatively similar to the noninteracting result [22]. The effects of the pulsed bias on the interference of the current in the DQD system are explored. The transient transport is driven by a pulsed bias potential $V(t)$. For simplicity, the ac pulsed bias is only added in the two leads. We consider two different pulsed biases: (i) upward pulse with $V_{\rm L} = V_{\rm R} = 0$ for $t < 0$ and $V_{\rm L} = -V_{\rm R} = V$ otherwise; (ii) downward pulse with $V_{\rm L} = -V_{\rm R} = V$ for $t < 0$ and $V_{\rm L} = V_{\rm R} = 0$ otherwise. By using the nonequilibrium Green's function method, the time-dependent current driven by the ac pulse can be calculated. We find that the oscillation behavior of the current has a clear dependence on the pulse bias and the interdot coupling strength. For the weak interdot coupling case, the rising and falling processes are symmetric in the linear bias regime, while quantum ringing in the time-dependent current appears for a large bias. For the strong interdot coupling case, the interference process is important and the current in the system shows the quantum beat. The quantum beat tends to disappear for large energy differences and high temperature.

The rest of this paper is organized as follows. In section 2, the theoretical formula for calculating the time-dependent current in the T-shaped DQD system is presented. In section 3, we show the numerical results along with some discussions. Finally, a brief summary is given in section 4.

2. Physical model and formula

In the T-shaped DQD structure, a central QD1 is connected to the two normal-metal leads while a side QD2 is coupled only to the central one. The Hamiltonian of the system can be described as follows:

$$H = \sum_{\alpha={\rm L,R}} H_\alpha + H_{\rm D} + H_{\rm T}, \tag{1}$$

with

$$H_\alpha = \sum_k \epsilon_{\alpha,k} a^\dagger_{\alpha,k} a_{\alpha,k}, \tag{2}$$

$$H_{\rm D} = \sum_{i=1,2} \varepsilon_i d_i^\dagger d_i - (t_{\rm c} d_1^\dagger d_2 + {\rm h.c.}), \tag{3}$$

$$H_{\rm T} = \sum_{\alpha,k} t_\alpha d_1^\dagger a_{\alpha,k} + {\rm h.c.} \tag{4}$$

H_α ($\alpha = {\rm L, R}$) describes the left and right normal-metal leads. $H_{\rm D}$ models the T-shaped double quantum dots where $d_i^\dagger$ (d_i) represents the creation (annihilation) operator of the electron with energy ε_i in QDi ($i = 1, 2$). $t_{\rm c}$ denotes the interdot coupling strength. $H_{\rm T}$ represents the tunneling coupling between the QD and leads, and the tunneling matrix elements are set as t_α. Under the adiabatic approximation [7, 8], the external time-dependent bias potential can be reflected in the single-electron energy $\epsilon_{\alpha,k}(t)$ which can be separated into two parts: $\epsilon_{\alpha,k}$ and $V_\alpha(t)$, where $\epsilon_{\alpha,k}$ is the time-independent single-electron energy and $V_\alpha(t)$ is the time-dependent part from the external time-dependent bias potential. $V_\alpha(t)$ is the step-like pulse with two different types: (i) upward pulse with $V_{\rm L} = V_{\rm R} = 0$ for $t < 0$ and $V_{\rm L} = -V_{\rm R} = V$ otherwise; (ii) downward pulse with $V_{\rm L} = -V_{\rm R} = V$ for $t < 0$ and $V_{\rm L} = V_{\rm R} = 0$ otherwise.

Using the Keldysh equation and the analytic continuation theory, the time-dependent current I_α from the α lead to the central region can be expressed in terms of the dot's Green's function as [7, 23]

$$I_\alpha(t) = \frac{2}{\hbar}\,{\rm Re}\int {\rm d}t'[\mathbf{G}^<(t,t')\mathbf{\Sigma}^{\rm a}_\alpha(t',t) + \mathbf{G}^{\rm r}(t,t')\mathbf{\Sigma}^<_\alpha(t',t)]. \tag{5}$$

The Green's functions are defined as $\mathbf{G}^{\rm r}(t,t') = -{\rm i}\theta(t-t')\langle\{\Psi(t), \Psi^\dagger(t')\}\rangle$ and $\mathbf{G}^<(t,t') = {\rm i}\langle\Psi^\dagger(t')\Psi(t)\rangle$ with the operator $\Psi = (d_1^\dagger, d_2^\dagger)^\dagger$. Thus, the Green's function $\mathbf{G}^{\rm r,<}$ and the self-energy $\mathbf{\Sigma}^{<,{\rm a}}$ are all two-dimensional matrices in the DQD system. Under the wide-band approximation, the retarded self-energy due to the α lead can be derived as

$$\mathbf{\Sigma}^{\rm r}_\alpha(t,t') = -\frac{\rm i}{2}\delta(t-t')\mathbf{\Gamma}_\alpha = -\frac{\rm i}{2}\delta(t-t')\begin{pmatrix}\Gamma_\alpha & 0\\ 0 & 0\end{pmatrix}, \tag{6}$$

where Γ_α is the coupling between the QD and the α lead defined by $\Gamma_\alpha = 2\pi\rho_\alpha t_\alpha^* t_\alpha$ with ρ_α being the density of states of the α lead. The advanced self-energy can be obtained from the relation $\mathbf{\Sigma}^{\rm a}_\alpha = (\mathbf{\Sigma}^{\rm r}_\alpha)^\dagger$. Similarly, the smaller self-energy due to the α lead can be derived as

$$\mathbf{\Sigma}^<_\alpha(t,t') = {\rm i}\int\frac{{\rm d}\epsilon}{2\pi}\exp\left[-{\rm i}\epsilon(t-t') - {\rm i}\int_{t'}^{t}{\rm d}t_1 V_\alpha(t)\right] \times f_\alpha(\epsilon)\mathbf{\Gamma}_\alpha, \tag{7}$$

where $f_\alpha(\epsilon) = 1/({\rm e}^{(\epsilon-\mu_\alpha)/k_{\rm B}T} + 1)$ is the Fermi distribution function of the α lead. With the self-energy obtained above, the lesser Green's functions can be calculated by using Keldysh equation $\mathbf{G}^<(t,t') = \int{\rm d}t_1\int{\rm d}t_2\mathbf{G}^{\rm r}(t,t_1)\mathbf{\Sigma}^<(t_1,t_2)\mathbf{G}^{\rm a}(t_2,t')$, where $\mathbf{G}^{\rm a} = (\mathbf{G}^{\rm a})^\dagger$ and $\mathbf{\Sigma}^<(t_1,t_2) = \sum_\alpha \mathbf{\Sigma}^<_\alpha(t_1,t_2)$. The Green's function $\mathbf{G}^{\rm r}(t,t')$ is the Fourier transformation of $\mathbf{G}^{\rm r}(\epsilon)$ with $\mathbf{G}^{\rm r}(t,t') = \int\frac{{\rm d}\epsilon}{2\pi}\exp[-{\rm i}\epsilon(t-t')]\mathbf{G}^{\rm r}(\epsilon)$. $\mathbf{G}^{\rm r}(\epsilon)$ can be derived from the Dyson equation $\mathbf{G}^{\rm r}(\epsilon) = [\mathbf{g}^{r-1}(\epsilon) - \mathbf{\Sigma}^{\rm r}(\epsilon)]^{-1}$, where $\mathbf{g}^{\rm r}(\epsilon)$ is the Green's function of the DQD system without the coupling to the leads

$$\mathbf{g}^{\rm r}(\epsilon) = \begin{pmatrix}\frac{1}{\epsilon-\varepsilon_1+{\rm i}0^+} & 0\\ 0 & \frac{1}{\epsilon-\varepsilon_2+{\rm i}0^+}\end{pmatrix}, \tag{8}$$

and $\mathbf{\Sigma}^{\rm r} = \sum_\alpha \mathbf{\Sigma}^{\rm r}_\alpha$. Substituting the retarded (advanced) Green's function and the lesser self-energy into the Keldysh formula and after some algebraic calculations, we can obtain

$$\mathbf{G}^<(t,t') = \int{\rm d}t_1\int{\rm d}t_2\mathbf{G}^{\rm r}(t,t_1)\mathbf{\Sigma}^<(t_1,t_2)\mathbf{G}^{\rm a}(t_2,t') = {\rm i}\int\frac{{\rm d}\epsilon}{2\pi}\sum_\alpha f_\alpha(\epsilon)\mathbf{A}_\alpha(\epsilon,t)\mathbf{\Gamma}_\alpha\mathbf{A}^\dagger_\alpha(\epsilon,t'), \tag{9}$$

where

$$\mathbf{A}_\alpha(\epsilon,t)=\int \mathrm{d}t' \exp\left[\mathrm{i}\epsilon(t-t')+\mathrm{i}\int_{t'}^{t}\mathrm{d}t_1 V_\alpha(t)\right]\mathbf{G}^{\mathrm{r}}(t,t'). \tag{10}$$

With the retarded and lesser Green's functions, the current becomes [8, 9, 24]

$$I_{\mathrm{L}}(t)=-\frac{e}{\hbar}\int\frac{\mathrm{d}\epsilon}{2\pi}\mathrm{Tr}\Big\{2f_{\mathrm{L}}(\epsilon)\,\mathrm{Im}[\mathbf{\Gamma}_{\mathrm{L}}\mathbf{A}_{\mathrm{L}}(\epsilon,t)] + \mathrm{Re}\Big[\mathbf{\Gamma}_{\mathrm{L}}\sum_\beta f_\beta(\epsilon)\mathbf{A}_\beta(\epsilon,t)\mathbf{\Gamma}_\beta\mathbf{A}_\beta^\dagger(\epsilon,t)\Big]\Big\}. \tag{11}$$

For the upward pulse with $V_{\mathrm{L}}=V_{\mathrm{R}}=0$ for $t<0$ and $V_{\mathrm{L}}=-V_{\mathrm{R}}=V$ for $t>0$, $\mathbf{A}_{\mathrm{LU}}(\epsilon)$ are

$$\begin{aligned}\mathbf{A}_{\mathrm{LU}}(\epsilon,t<0)&=\mathbf{G}^{\mathrm{r}}(\epsilon),\\ \mathbf{A}_{\mathrm{LU}}(\epsilon,t>0)&=\mathbf{G}^{\mathrm{r}}(\epsilon+V_{\mathrm{L}})+\mathrm{e}^{\mathrm{i}V_{\mathrm{L}}t}\int_t^\infty \mathrm{d}t'\mathrm{e}^{\mathrm{i}\epsilon t'}\mathbf{G}^{\mathrm{r}}(t')\\ &\quad-\int_t^\infty \mathrm{d}t'\mathrm{e}^{\mathrm{i}(\epsilon+V_{\mathrm{L}})t'}\mathbf{G}^{\mathrm{r}}(t').\end{aligned} \tag{12}$$

For the downward pulse with $V_{\mathrm{L}}=-V_{\mathrm{R}}=V$ for $t<0$ and $V_{\mathrm{L}}=V_{\mathrm{R}}=0$ for $t>0$, $\mathbf{A}_{\mathrm{LD}}(\epsilon,t)$ are

$$\begin{aligned}\mathbf{A}_{\mathrm{LD}}(\epsilon,t<0)&=\mathbf{G}^{\mathrm{r}}(\epsilon+V_{\mathrm{L}}),\\ \mathbf{A}_{\mathrm{LD}}(\epsilon,t>0)&=\mathbf{G}^{\mathrm{r}}(\epsilon)+\mathrm{e}^{-\mathrm{i}V_{\mathrm{L}}t}\int_t^\infty \mathrm{d}t'\mathrm{e}^{\mathrm{i}(\epsilon+V_{\mathrm{L}})t'}\mathbf{G}^{\mathrm{r}}(t')\\ &\quad-\int_t^\infty \mathrm{d}t'\mathrm{e}^{\mathrm{i}\epsilon t'}\mathbf{G}^{\mathrm{r}}(t').\end{aligned} \tag{13}$$

The expressions for $\mathbf{A}_{\mathrm{RU}}$ and $\mathbf{A}_{\mathrm{RD}}$ can be obtained from equations (12) and (13) by changing V_{L} to V_{R}.

In the small pulse bias V_{L} limits we can expand $\mathbf{A}_{\mathrm{L}}(\epsilon,t)$ to the first order of V_{L} as $\mathbf{A}_{\mathrm{L}}(\epsilon,t)=\mathbf{A}_{\mathrm{L}}(\epsilon,0)+V_{\mathrm{L}}\mathbf{A}_{\mathrm{L}}^1(\epsilon,t)$ with $\mathbf{A}_{\mathrm{L}}^1$ expressed as

$$\begin{aligned}\mathbf{A}_{\mathrm{LU}}^1(\epsilon,t>0)&=\mathrm{i}t\int_t^\infty \mathrm{d}t'\mathrm{e}^{\mathrm{i}\epsilon t'}\mathbf{G}^{\mathrm{r}}(t')\\ &\quad+\mathrm{i}\int_0^t \mathrm{d}t'\mathrm{e}^{\mathrm{i}\epsilon t'}t'\mathbf{G}^{\mathrm{r}}(t'),\end{aligned} \tag{14}$$

and

$$\begin{aligned}\mathbf{A}_{\mathrm{LD}}^1(\epsilon,t>0)&=-\mathrm{i}t\int_t^\infty \mathrm{d}t'\mathrm{e}^{\mathrm{i}\epsilon t'}\mathbf{G}^{\mathrm{r}}(t')\\ &\quad-\mathrm{i}\int_0^t \mathrm{d}t'\mathrm{e}^{\mathrm{i}\epsilon t'}t'\mathbf{G}^{\mathrm{r}}(t').\end{aligned} \tag{15}$$

The current can also be expanded as $I_{\mathrm{L}}(t)=I_{\mathrm{L}}(0)+V_{\mathrm{L}}X_{\mathrm{L}}(t)$ with

$$\begin{aligned}X_{\mathrm{L}}(t)=-\frac{e}{\hbar}\int\frac{\mathrm{d}\epsilon}{2\pi}\mathrm{Tr}\Big\{&2f_{\mathrm{L}}(\epsilon)\,\mathrm{Im}[\mathbf{\Gamma}_{\mathrm{L}}\mathbf{A}_{\mathrm{L}}^1(\epsilon,t)]\\ &+\mathrm{Re}\,\mathbf{\Gamma}_{\mathrm{L}}\sum_\beta f_\beta(\epsilon)[\mathbf{A}_\beta^1(\epsilon,t)\mathbf{\Gamma}_\beta(\mathbf{G}^{\mathrm{r}}(\epsilon))^\dagger\\ &+\mathbf{G}^{\mathrm{r}}(\epsilon)\mathbf{\Gamma}_\beta(\mathbf{A}_\beta^1(\epsilon,t))^\dagger]\Big\},\end{aligned} \tag{16}$$

where $X_{\mathrm{L}}(t)$ is the first-order expansion coefficient with respect to the bias V_{L}.

3. Numerical results and discussions

In the numerical calculation, we set $\hbar=e=1$ and the coupling $\Gamma=\Gamma_{\mathrm{L}}+\Gamma_{\mathrm{R}}=1$ as an energy unit. The temperature is set as zero except for the discussion about the temperature effects. The system is in a steady state at $t<0$ and the current is time independent. At $t=0$, the bias is abruptly turned on (off) for the upward (downward) pulse case. After that, the system begins to relax, and finally the system enters into a new steady state. Thus in the following discussion we only plot the current $I_{\mathrm{L}}(t)$ and the related quantities for $t>0$. To make the physical picture clear, the two coupled QD levels can be diagonalized into the decoupled antibonding (+) and bonding (−) states with energy $\varepsilon_\pm=\frac{1}{2}[\varepsilon_1+\varepsilon_2\pm\sqrt{(\varepsilon_1-\varepsilon_2)^2+4t_{\mathrm{c}}^2}]$. The linewidth matrix corresponding to the two states coupled to the α lead are, respectively, $\Gamma_+^\alpha=\Gamma_1^\alpha\cos^2\beta$ and $\Gamma_-^\alpha=\Gamma_1^\alpha\sin^2\beta$, where $\beta(t)=1/2\tan^{-1}[2t_{\mathrm{c}}/(\varepsilon_1-\varepsilon_2)]$. Therefore, the DQD system is mapped onto a system of two independent molecular states with band $\Gamma_\pm^\alpha$ connected to the leads.

First of all we study the case of weak interdot coupling at $t_{\mathrm{c}}=0.01$. The energy levels of the two QDs are set as $\varepsilon_1=\varepsilon_2=0$. Then, the bonding and antibonding states are at $\varepsilon_-=-t_{\mathrm{c}}$ and $\varepsilon_+=t_{\mathrm{c}}$, respectively. Since t_{c} is very small, the two state levels can be approximately viewed as $\varepsilon_+\approx\varepsilon_-=\varepsilon_0$. For the small pulse bias V limit, the instantaneous current $I_{\mathrm{L}}(t)$ can be expanded as $I_{\mathrm{L}}(t)=I_{\mathrm{L}}(0)+X_{\mathrm{L}}(t)V_{\mathrm{L}}$. The first-order expansion parameters $X_{\mathrm{LU/D}}(t)$ of the currents $I_{\mathrm{LU/D}}(t)$ versus time t are plotted in figure 1(a). It is seen that the expanding parameters $X_{\mathrm{L}}(t)$ for the upward and downward pulses are symmetric as $X_{\mathrm{LU}}(t)=-X_{\mathrm{LD}}(t)$. The current $I_{\mathrm{LU}}(t)$ and $I_{\mathrm{LD}}(t)$ responding to the upward and downward pulses are also symmetric as shown in figure 1(b). As time t increases, $I_{\mathrm{LU/D}}(t)$ deviates from the initial value $I_{\mathrm{LU/D}}(0)$. For the upward (downward) pulse, the current increases (decreases) and the device is gradually turned on (off). As a result, the instantaneous current shows a clear increase (decrease) before reaching the new steady state for the upward (downward) pulse. It means that in the linear (small) bias regime, the upward pulse is the reversal process of the downward pulse, so that the turn-on time is the same as the turn-off time.

Figure 2 depicts the currents I_{LU} and I_{LD} versus time t for various large pulse biases V. The current responses to the upward and downward pulses are asymmetric at the large bias V, which is quite different from the case of small bias. It is seen that the decreasing process of the current I_{LD} in the large bias case is much stronger than that of the small bias case. In this nonlinear regime, the upward and downward processes are asymmetric and the turn-on time is much larger than the turn-off time. What is more interesting is that the current I_{LU} in the large bias case oscillates with increasing time t, while the amplitude of the oscillation decreases and finally vanishes. The oscillation frequency and period depend on the bias V, which can be expressed as $\omega=|V-\varepsilon_0|$ and $T=2\pi/|V-\varepsilon_0|$, respectively. The damping of the oscillation amplitude is due to the lead–dot coupling Γ, and the damping time is about $1.0(2\pi/\Gamma)$. This oscillation does not appears in the small bias case, because the frequency is too small and the current cannot show the oscillations before the system is completely relaxed.

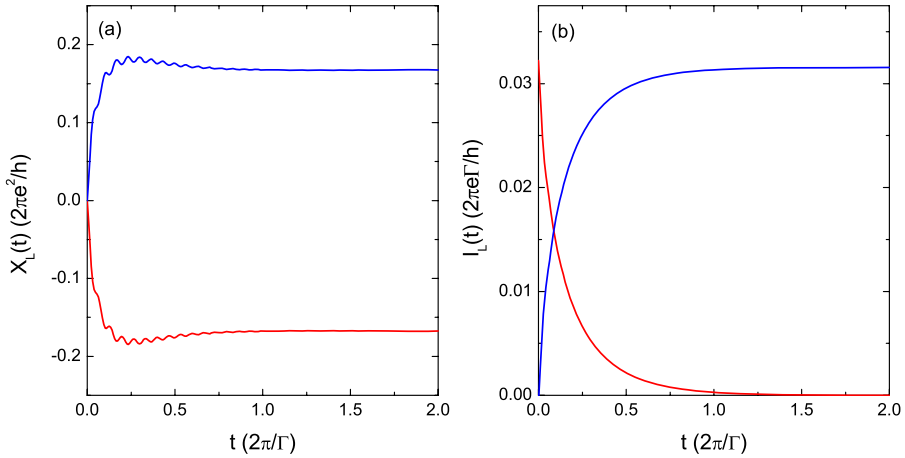

Figure 1. The first-order expansion coefficients $X_{\rm LU}(t)$ and $X_{\rm LD}(t)$ (a) and the currents $I_{\rm LU}(t)$ (blue) $I_{\rm LD}(t)$ (red) (b) versus time t for the upward and downward pulse bias cases. The parameters are $t_{\rm c} = 0.01$ and $V = 0.1$.

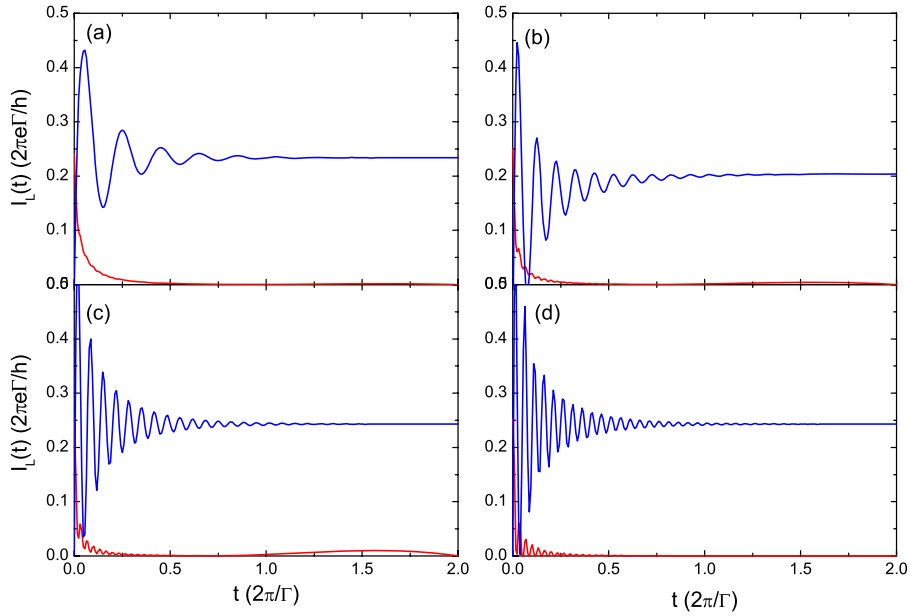

Figure 2. The currents $I_{\rm LU}(t)$ (blue) and $I_{\rm LD}(t)$ (red) versus time t for weak interdot coupling $t_{\rm c} = 0.01$ at different biases of (a) $V = 5$, (b) $V = 10$, (c) $V = 15$, and (d) $V = 20$.

With increasing V, the oscillation frequency also increases, and thus the current oscillations can appear clearly.

Next, we discuss the case of strong interdot coupling. Figure 3 shows the time evolution of the current $I_{\rm LU}$ for various large interdot couplings. It is seen that the currents present the typical quantum beat character, which is absent in the weak interdot coupling case. In particular, more beats appear in the current as $t_{\rm c}$ increases. The quantum beating is caused by interference between tunneling electrons through the two QDs. In this T-shaped DQD structure, there are two paths for tunneling electrons. One is the N–QD1–N path and the other is N–QD1–QD2–QD1–N. In the presence of strong interdot coupling $t_{\rm c}$, the frequency ω becomes dependent on interdot coupling as $\omega_{\pm} = |V - \varepsilon_0 \pm t_{\rm c}|$. The total current can be viewed as being composed of two components: I_+ and I_- contributed by electrons tunneling through the channels ε_+ and ε_-. Furthermore, I_+ and I_- oscillate with different frequencies of ω_+ and ω_+. Therefore, the interference of these two current components results in quantum beats with beat frequency given by $|\omega_+ - \omega_-| = 2t_{\rm c}$. Since both I_+ and I_- start from zero at $t = 0$, the total current reaches its first node soon due to this strong initial condition. Only part of the quantum beat appears in the current before the first node. After this, the whole period of the quantum beats can appear in the current. The interplay between oscillation amplitudes and decay rates gives rise to other nodes in the total current. The quantum beats cannot be seen for weak $t_{\rm c}$ because the frequencies of the two components of the currents almost coincide. This means that the appearance of the quantum beats in the currents can be tuned by the interdot coupling strength $t_{\rm c}$. It is also seen that the relaxation of the quantum beats is different for different interdot couplings, since the beat frequency depends

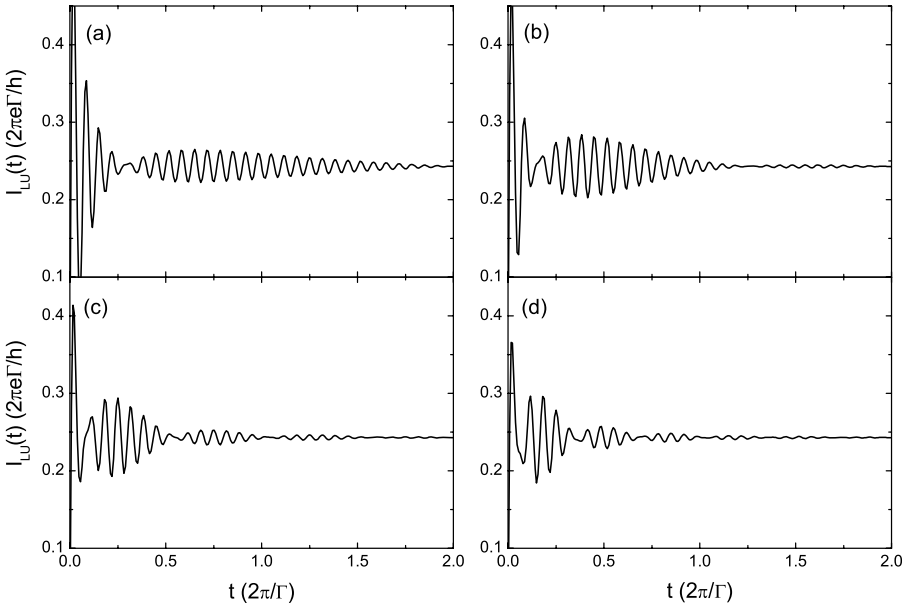

Figure 3. The currents $I_{\mathrm{LU}}(t)$ versus time t at $V = 15$ for different interdot couplings of (a) $t_{\mathrm{c}} = 0.25$, (b) $t_{\mathrm{c}} = 0.5$, (c) $t_{\mathrm{c}} = 1.0$ and (d) $t_{\mathrm{c}} = 1.5$.

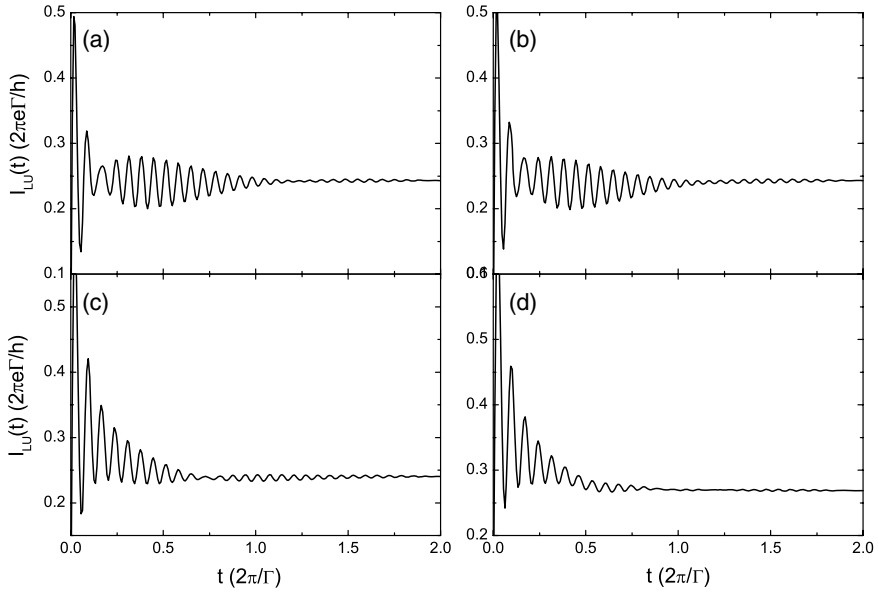

Figure 4. The currents $I_{\mathrm{LU}}(t)$ versus time t at $t_{\mathrm{c}} = 0.5$ and $V = 15$ for different energy differences of (a) $\Delta\varepsilon = 0.1$, (b) $\Delta\varepsilon = 0.2$, (c) $\Delta\varepsilon = 1.0$ and (d) $\Delta\varepsilon = 2.0$.

on t_{c} as mentioned above. This is quite different from the case of quantum ringing, in which the relaxation only depends on the coupling strength Γ.

The energy difference $\Delta\varepsilon$ between QD1 and QD2 also has a distinct influence on the quantum beats. Figure 4 shows the current I_{LU} versus time t for various $\Delta\varepsilon$. With increasing $\Delta\varepsilon$, the quantum beat behavior is greatly suppressed. The current only shows quantum ringing for large enough $\Delta\varepsilon$. The reason for this is related to the linewidth Γ_+ and Γ_- of the antibonding and bonding states. When $\Delta\varepsilon$ increases from zero, β deviates from $\pi/4$. Therefore, Γ_- and Γ_+ become inequivalent, which greatly suppresses the interference between the two molecular states. Then the quantum beat is destroyed by the large energy difference. In figure 5, the currents I_{LU} and I_{LD} versus time t for various pulsed biases V are plotted. As the bias V increases, the current I_{LU} oscillates much more rapidly and more quantum ringing appears. The reason is that the frequency of the quantum ringing is proportional to the bias V as mentioned above. However, the period of the quantum beat does not change, because the frequency of the quantum beat depends on the interdot coupling t_{c} but not on the bias. For the current I_{LD}, the decreasing process becomes much stronger for the large bias than that for the small bias.

Finally, we discuss the effects of the temperature $k_{\mathrm{B}}T$ on the quantum beat. In figure 6, we plot the influence of various temperatures on the quantum coherent beat of the

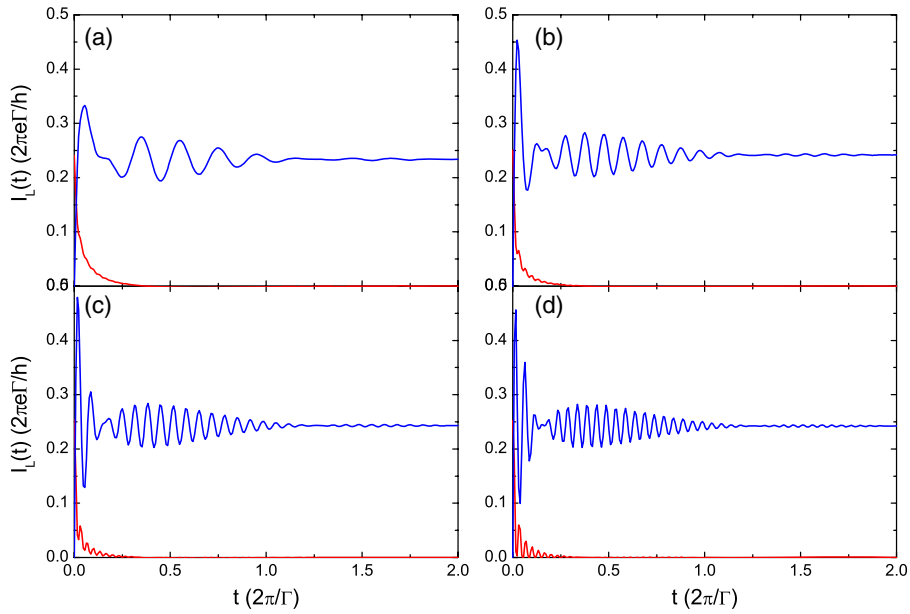

Figure 5. The currents $I_{\mathrm{LU}}(t)$ (blue) and $I_{\mathrm{LD}}(t)$ (red) versus time t for strong interdot coupling $t_{\mathrm{c}} = 0.5$ at different biases of (a) $V = 5$, (b) $V = 10$, (c) $V = 15$ and (d) $V = 20$.

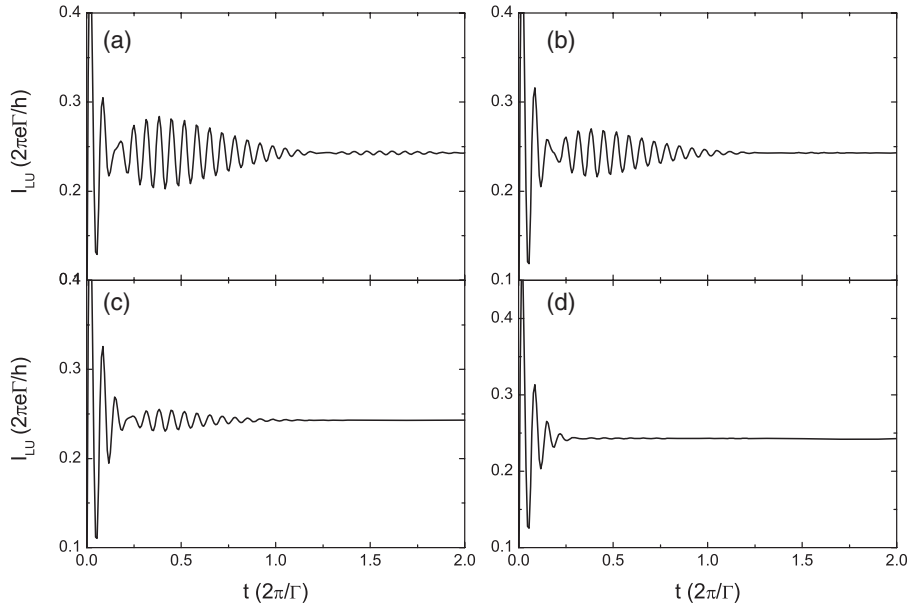

Figure 6. The currents $I_{\mathrm{LU}}(t)$ versus time t at $t_{\mathrm{c}} = 0.5$ and $V = 15$ for different temperatures (a) $k_{\mathrm{B}}T = 0.01$, (b) $k_{\mathrm{B}}T = 0.1$, (c) $k_{\mathrm{B}}T = 0.2$ and (d) $k_{\mathrm{B}}T = 0.5$.

currents. Coherent quantum beats can be clearly seen for both $k_{\mathrm{B}}T = 0.01$ and 0.1, but the beats are only residually observed for $k_{\mathrm{B}}T = 0.2$. As $k_{\mathrm{B}}T$ increases to 0.5, the quantum beat behavior tends to disappear in the current. When the temperature increases to $k_{\mathrm{B}}T \sim \Gamma$, the coherent oscillations of the quantum ringing and beats of the current are both strongly suppressed. The reason for this is related to the coherence loss caused by the high temperature. In general, quantum coherence is established at temperatures lower than the coupling strength as $k_{\mathrm{B}}T \ll \Gamma$. At this low temperature, the coherent resonant tunneling dominates and the electrons keep the coherence. The oscillation period of the current is much smaller than the damping time which depends only on the coupling strength. Then the current clearly shows the coherent oscillation. When the temperature increases to become comparable with Γ, the inelastic tunneling makes a large contribution, and the tunneling process becomes incoherent [25]. At the same time, the QD energy level is broadened by the high temperature and the damping time is greatly decreased. Thus the oscillations of the current I_+ and I_- are suppressed by the high temperature. As a result, both the quantum ringing and beats of the total current can be washed out as the temperature increases to exceed the coupling strength [12].

4. Conclusion

The quantum coherent ringing and beat of the current flowing through a T-shaped double quantum dot are theoretically studied. The time-dependent transport is calculated via a nonequilibrium Green's function in the transient after a bias voltage is turned on or off. The quantum coherent ringing and beat can be controlled by the interdot coupling and the pulsed bias. In the weak interdot coupling case, quantum ringing appears in the current only at large bias. The frequency of the quantum ringing increases as the bias increases. In the strong interdot coupling case, quantum beating appears in the current at large bias, but is absent in the weak interdot coupling case. With increasing interdot coupling, more quantum beats appear, since the beat frequency depends on the interdot coupling. Furthermore, the quantum beat behavior can be greatly suppressed by the large energy difference between the two quantum dots. Additionally, quantum ringing and quantum beats tend to disappear at high temperature.

Acknowledgments

This work is supported by the National Natural Science Foundation of China (grant no. 10704005), and the Beijing Municipal Science and Technology Commission (grant no. 2007B017).

References

[1] Fujiwara A, Takahashi Y and Murase K 1997 *Phys. Rev. Lett.* **78** 1532
[2] Kouwenhoven L P, Jauhar S, Orenstein J, Nagamune Y, Motohisa J and Sakaki H 1994 *Phys. Rev. Lett.* **73** 3443
[3] Blick R H, Haug R J, van der Weide D W, von Klitzing K and Eberl K 1995 *Appl. Phys. Lett.* **67** 3924
[4] Li S, Yu Z, Yen S F, Tang W C and Burke P J 2004 *Nano Lett.* **4** 753
[5] Plihal M, Langreth D C and Nordlander P 2000 *Phys. Rev.* B **61** R13341
[6] Schiller A and Hershfield S 2000 *Phys. Rev.* B **62** R16271
[7] Wingreen N S, Jauho A P and Meir Y 1993 *Phys. Rev.* B **48** 8487
[8] Jauho A P, Wingreen N S and Meir Y 1994 *Phys. Rev.* B **50** 5528
[9] Xing Y, Sun Q F and Wang J 2007 *Phys. Rev.* B **75** 125308
[10] Maciejko J, Wang J and Guo H 2006 *Phys. Rev.* B **74** 085324
[11] Zhu Y, Maciejko J, Ji T, Guo H and Wang J 2005 *Phys. Rev.* B **71** 075317
[12] Souza F M 2007 *Phys. Rev.* B **70** 205315
[13] Holleitner A W, Blick R H, Httel A K, Eberl K and Kotthaus J P 2002 *Science* **297** 70
[14] Kubala B and Konig J 2002 *Phys. Rev.* B **65** 245301
[15] de Guevara M L L, Claro F and Orellana P A 2003 *Phys. Rev.* B **67** 195335
[16] Drexler H, Scott J S, Allen S J, Campman K L and Gossard A C 1995 *Appl. Phys. Lett.* **67** 2816
[17] Oosterkamp T H, Fujisawa T, van der Wiel W G, Ishibashi K, Hijman R V, Tarucha S and Kouwenhoven L P 1998 *Nature* **395** 873
[18] Stoof T H and Nazarov Yu V 1996 *Phys. Rev.* B **53** 1050
[19] Hazelzet B L, Wegewijs M R, Stoof T H and Nazarov Yu V 2001 *Phys. Rev.* B **63** 165313
[20] Stafford C A and Wingreen N S 1996 *Phys. Rev. Lett.* **76** 1916
[21] Sato M, Aikawa H, Kobayashi K, Katsumoto S and Iye Y 2005 *Phys. Rev. Lett.* **95** 066801
[22] Arrachea L, Yeyati A L and Martin-Rodero A 2008 *Phys. Rev.* B **77** 165326
[23] Pan H and Lin T H 2006 *Phys. Rev.* B **74** 235312
[24] Pan H and Lin T H 2006 *Phys. Lett.* A **360** 317
Pan H, Zhao L N and Rong Lu 2008 *Physica* E **40** 2988
[25] Rokhinson L P, Guo L J, Chou S Y, Tsui D C, Eisenberg E, Berkovits R and Altshuler B L 2002 *Phys. Rev. Lett.* **88** 186801